

A low-blank photochemical extraction system for concentration and isotopic analyses of marine dissolved organic carbon

Steven R. Beaupré¹, Ellen R. M. Druffel, and Sheila Griffin

¹2212 Croul Hall, Department of Earth System Science, University of California Irvine, Irvine, CA, 92697-3100

Abstract

We report the development of a modified, low blank, ultraviolet oxidation and vacuum line system to convert marine dissolved organic carbon into carbon dioxide for concentration, $\Delta^{14}\text{C}$, and $\delta^{13}\text{C}$ analyses. The system performs quantitatively and precisely with preservation of isotopic signatures ($\pm 3\text{‰}$) based on additions of pure International Atomic Energy Agency standards. Analytical blank reduction from $< 1.5 \mu\text{M}$ to $0.2 \mu\text{M}$ enabled a decreased detection limit from a sample size of $\sim 650 \text{ mL}$ to 30 mL using a simple dilution technique. Combined with advances in analyses of ultra-small ($2 \mu\text{gC}$) samples using accelerator mass spectrometry, the technique provides a means for measuring $\Delta^{14}\text{C}$ values in samples that were previously not analyzable.

Dissolved organic carbon (DOC), operationally defined as the carbon contained in that fraction of organic matter in water which passes through a $0.2\text{--}1 \mu\text{m}$ filter, is the largest pool (ca. $0.6 \times 10^{18} \text{ g C}$) of organic matter in the oceans and is approximately equal in size to atmospheric CO_2 (Hedges 1992). Despite its abundance in the global carbon cycle and nearly a century of research, the majority ($> 60\% - 80\%$) of DOC has remained molecularly uncharacterized (Hedges 1992) and its biogeochemical fluxes incompletely resolved. Global riverine input of $\sim 0.2 \text{ Gt DOC per year}$ (Meybeck 1982) is sufficient to support its radiocarbon (^{14}C) based oceanic residence time, yet composition (Meyers-Schulte and Hedges 1986; Opsahl and Benner 1997) and stable carbon (^{13}C) isotopic signature (Williams and Gordon 1970) measurements suggest the majority of marine DOC is autochthonous, ultimately originating from primary production in the euphotic zone. Furthermore, while the $4000 - 6000 \text{ y } ^{14}\text{C}$ ages reported

for deep marine DOC suggest that a major proportion cycles on very long time scales and ages in situ during deep water transit (Bauer et al. 1992; Williams and Druffel 1987), the source of apparent chemical resilience and the removal processes necessary to produce these ages remain unknown. The published body of $\Delta^{14}\text{C}$ values has been critical to understanding marine DOC biogeochemistry, yet it contains relatively few measurements because of methodological difficulties associated with low DOC concentrations, an overwhelming proportion of salts, and high blanks.

The marine DOC ultraviolet (UV) extraction method (Armstrong et al. 1966; Williams 1968; Williams and Gordon 1970; Williams et al. 1969), and subsequent refinements (Bauer et al. 1998a; Druffel et al. 1989) that co-evolved with smaller sample size requirements of accelerator mass spectrometry (AMS) ^{14}C measurement, has been particularly well-suited for isotopic analysis of marine DOC. It is amenable to batch reactors capable of oxidizing the large seawater aliquots required to collect enough DOC for isotopic analysis. It is a minimally invasive technique, involving only acidification and sparging of dissolved inorganic carbon (DIC) from filtered seawater prior to photochemical oxidation of DOC to CO_2 , thus minimizing the risk of contamination. Lastly, replicate analyses by Bauer et al. (1998a) demonstrated that good reproducibility (with single standard deviations of $\pm 1 \mu\text{M}$ and $\pm 3\text{‰}$ to 6‰ for concentration and $\Delta^{14}\text{C}$ measurements, respectively) accompanies low blanks ($< 1.5 \mu\text{M}$). Based on these techniques, a modified method for UV extraction of bulk marine nonvolatile DOC for isotopic analysis has been developed using simple, novel devices to decrease the analytical blank to $\sim 0.2 \mu\text{M}$, and reduce the

Acknowledgments

We graciously acknowledge the expertise, assistance, and endless patience of the following contributors: Dr. John Southon and Dr. Guaciara dos Santos of the UCI KCCAMS laboratory for their assistance in measuring isotope ratios; Dr. Don Blake, Dr. Simone Meinardi, and Gloria Liu for chromatographic characterization of trace gases in our samples; Dr. Ken Smith for generously sharing ship-time; Bob Wilson for sample collection assistance; the captain and crew of the R/V *New Horizon*; and Jorg Meyer, UCI's scientific glassblower. This material is based upon work supported under a National Science Foundation (NSF) Graduate Research Fellowship, and NSF grants OCE-0137207 and OCE-0526463 (to E. R. M. Druffel). Any opinions, findings, conclusions, or recommendations expressed in this presentation are those of the authors and do not necessarily reflect the views of the National Science Foundation.

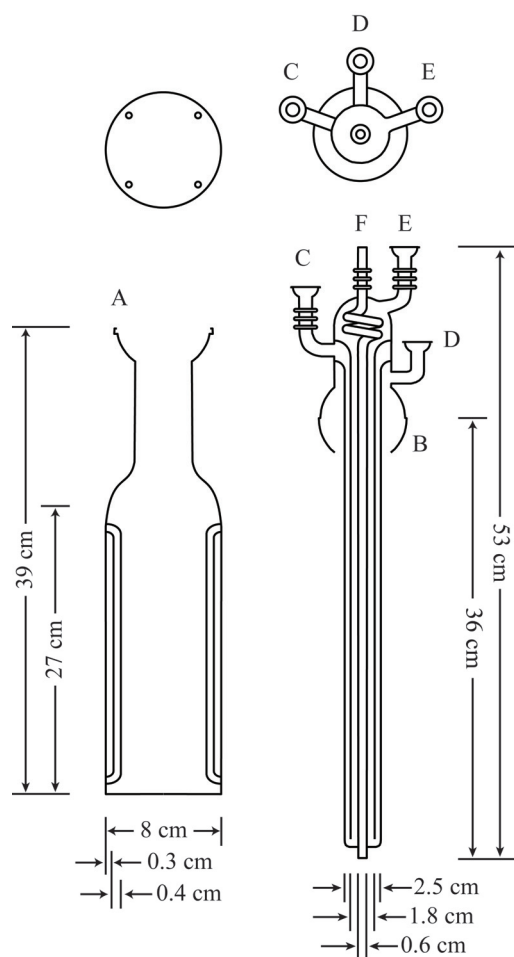


Fig. 1. The photochemical reactor. Quartz reactor body (bottom left) with a cross-sectional view (top left) showing the baffle rod positions. Pyrex heat exchanger (bottom right) with an overhead view (top right) illustrating locations of the (C) cold-water return, (D) vent to DOC line, and (E) cold-water supply 18/9 SJ sockets. Other components include the (A) 65/40 SJ socket, (B) 65/40 SJ ball member, and (F) helium supply connection. See text for additional details.

detection limit while minimizing potential hazards to the system operator. Using this methodology combined with recent advances in small sample AMS analysis (Santos et al. 2007), the minimum natural seawater sample size required for reliable DOC $\Delta^{14}\text{C}$ analysis is reduced from 650 mL (Bauer et al. 1998a) to ~30 mL by a simple dilution technique using the same reactor with similar performance.

Materials and procedures

Sample collection—The data presented are, in part, from analyses of samples collected aboard the R/V *New Horizon* during the Pulse 45 cruise to the NE Pacific, 24 October–3 November 2004. Samples were collected at Station M (34°50' N, 123°00' W), a long-term abyssal study site established June 1989 that is located 220 km west of Point Conception, California (Smith and Druffel 1998).

Seawater samples were collected using a CTD rosette of 24 ten-liter Niskin bottles. All Niskin bottles were scrubbed with warm soapy water and thoroughly rinsed on deck prior to leaving port. During sampling, the bottles were thoroughly flushed with seawater prior to tripping. Seawater was gravity filtered directly from the bottles through 0.2 μm Whatman Polycap AS filter capsules that were pre-rinsed with acetonitrile and Milli-Q water, and Nalgene 50 platinized silicone tubing previously washed with 10% HCl and Milli-Q water. The filter and tubing assembly were flushed with sample for several minutes prior to dispensing into one-gallon glass jugs (Fisher Scientific). The jugs, which were previously cleaned with warm-soapy water, 10% HCl, and deionized water followed by baking at 550°C for 2 h in a muffle furnace, were rinsed three times with seawater before filling to ~85% capacity. The jugs were then sealed with cleaned polytetrafluoroethylene (PTFE) Teflon lined caps, wrapped in clean polypropylene bags, and stored frozen at -20°C.

Photochemical reactor—The reactor body is a custom, 8-cm outer diameter (OD), UV-transparent vitreous silica (Vitreosil, Thermal American Fused Quartz) cylinder, necked down to a 65/40 spherical joint (SJ) socket member (Fig. 1). The flat bottom of the reactor was formed by fusing a quartz disk onto the cylinder to ensure a smooth platform for agitation with a custom Pyrex-encased magnetic spinbar (Fig. 2). Four evenly spaced, vertical, 4 mm diameter solid quartz baffle rods ensure thorough, turbulent mixing of the entire seawater sample. Since the horizontal cross-section of the reactor is uniform throughout the working height of the reactor, it has been calibrated for measuring sample volume. This is quantified by supporting and leveling the reactor in a custom ring stand equipped with a clear vertical ruler, measuring the water height to the nearest 0.5 mm, and calculating the volume based on calibration to ± 3 mL. The reactor body was designed to contain approximately 1 L seawater when assembled with a heat exchanger.

The Pyrex heat exchanger is a cold-finger condenser, coaxial to a central stem that ends in a medium porosity frit to deliver helium into the reactor (Fig. 1). It was manufactured with a two-coil helix on the helium delivery tubing inside of the heat

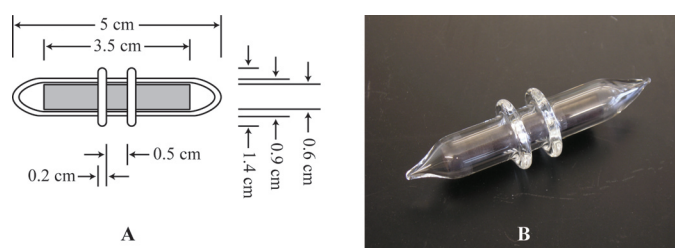


Fig. 2. Schematic (A) and photograph (B) of a custom Pyrex encased magnetic spinbar. Two marias allow the bar to pivot without tipping, reduce frictional grinding, and prolong its lifetime. A small gap between the magnet (~0.6 cm OD) and inner wall of the glass casing (0.7 cm ID) eliminates fracturing due to differential thermal expansion, making these spinbars suitable for high temperature operation or cleaning by baking to 550°C.

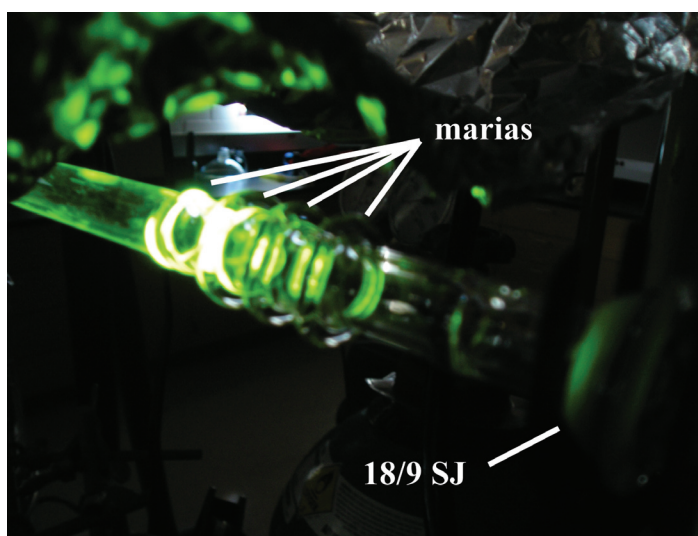


Fig. 3. A photograph of light from the UV lamp (originating from left) channeling through glass tubing, which is largely dissipated by marias before reaching the o-ring sealed 18/9 spherical joint. See text for additional details.

exchanger to minimize stresses on the glass generated by thermal gradients during irradiation. The helium tubing terminates in a fire-polished 6 mm OD tube that connects to gas supply tubing using an Ultra-Torr (Swagelok) fitting. The glass 18/9 SJ sockets connect to the recirculating chiller's (Neslab CFT-25) cooling water supply and return line's braided clear polyvinyl chloride (PVC) tubing (Nalgene) using 18/9 SJ o-ring ball-member hose-barbed adapters and stainless steel screw-lock pinch clamps. All joints sealed by Viton o-rings in the vicinity of the lamp are fitted with 3 solid glass rings around the circumference of the tubing, known as marias (Hammesfahr and Strong 1968), which act to dissipate energy propagated through the tubing (Fig. 3), thereby prolonging the o-rings' useful lifetime, ensuring reliable seals and, most importantly, reducing the contribution of o-ring degradation to the blank. Since the large 65/40 SJ and smaller vent 18/9 SJ do not contain o-rings, they are lubricated with 85% H_3PO_4 and secured with stainless steel screw-lock pinch clamps. This overall design was intended to maximize the glassware's durability and ease of use without compromising the security of any joints.

UV-lamp reflector assembly & cabinet—A six-inch, 1200 watt, medium pressure mercury arc UV lamp (UV Doctor) is supported vertically on insulating ceramic stand-offs at the primary focus of a custom aluminum elliptical reflector (Fig. 4) lined with highly polished Alzak aluminum sheeting (supplied by Hanovia, New Jersey). The lamp is clamped sufficiently taut to the stand-offs to safely secure it while compensating for thermal expansion and contraction during irradiation. The reflector's face is 11 cm wide by 25 cm high, and in cross-section, approximately traces the ellipse $(x/6.8 \text{ cm})^2 + (y/5.6 \text{ cm})^2 = 1$ with the primary focus located 2.9 cm from its vertex. This arrangement focuses light emitted from the lamp onto a

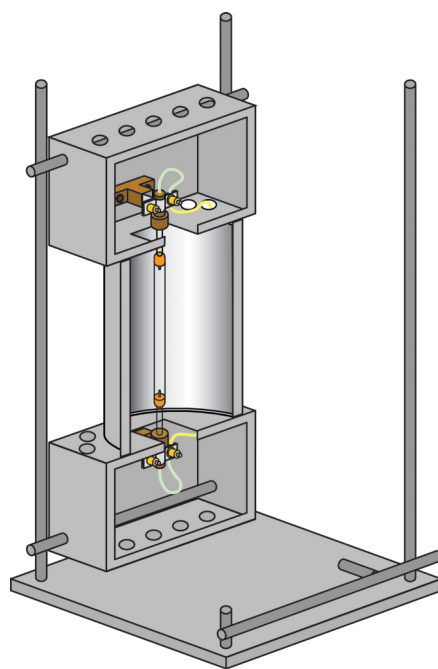


Fig. 4. UV lamp reflector assembly. The assembly is mounted on an aluminum stand with four 1.3 cm OD vertical support rods anchored into the vertices of a 24 cm \times 24 cm \times 1.3 cm base plate. Two of these rods support the reflector using lattice connector clamps (Chemglass Inc, not shown), one supports the neck of the reactor with a three-pronged clamp, and the fourth supports a framework to precisely align and restrain the magnetic spin plate (not shown) upon which the reactor rests. Ceramic stand-offs and the ceramic end-fittings of the lamp are shown in brown.

vertical line 5 cm in front of the reflector's face. However, the nearest wall of the quartz reactor has been positioned 3.5 cm from the reflector to minimize the photon path length and reflective losses on the curved glass surface while maintaining proper cooling of the lamp.

The assembly and reactor are housed in a cabinet made from lightweight steel trash cans (Fig. 5), designed primarily to (1) adequately cool the lamp using ambient air as a heat exchanging fluid, (2) safely vent noxious gases (e.g., O_3) produced during irradiation, and (3) protect the system operator from UV light. These objectives were met using four light-reducing baffled air intakes near the base of the cabinet and exhausting through a 5-inch inner diameter (ID) flame-retardant blended plastic/rubber duct hose (McMaster-Carr) to the laboratory fume hood. The interior of each intake box is painted black and partitioned such that air flows along a tightly folded path that extinguishes photons through absorption and scattering. Muffin fans fitted to the terminus of the exhaust duct provided the approximately 200 cfm ideal air-flow for cooling the lamp. This arrangement of drawing air through the cabinet from the exhaust, rather than forcing it through from the intakes, ensures a negative pressure within the system, and minimizes leakage of noxious gases (e.g., O_3).

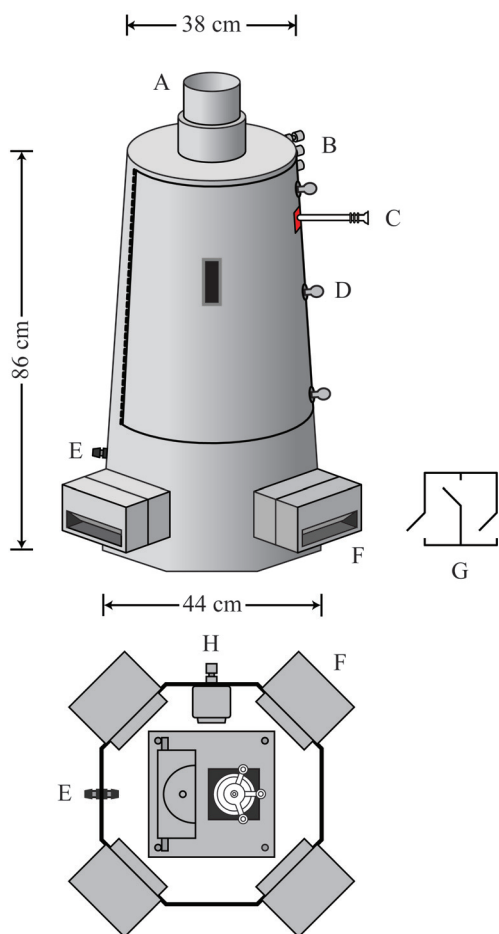


Fig. 5. Reactor cabinet (top) with footprint (bottom): (A) exhaust duct coupling; (B) bulkhead fittings for cooling water supply/return lines and helium supply line; (C) 12 mm OD Pyrex tubing connecting the reactor to DOC vacuum line via an 18/9 SJ with 3 marias, breaching the cabinet via a silicone flange (shown red); (D) one of three pawl latches securing the curved door, hinged on the left hand side; (E) bulkhead fitting for UV-lamp power lines; (F) light-reducing baffled air intakes; (G) cross-section of (F), illustrating the tightly folded path that cooling air must travel; (H) electrical outlet box and bulkhead fitting. See text for additional details.

Further protection from UV light was implemented as follows. All tubing and wires breach the cabinet walls via bulkhead fittings (Swagelok) and all permanent seams on the cabinet's surface were sealed with high-temperature flue tape (3M Corporation) to eliminate light-leakage through small gaps. Glass tubes connecting the reactor to the helium supply and the vacuum line exit the cabinet via flexible silicone flanges backed with aluminum foil. These materials provide a tight seal that can withstand the energy emitted from the lamp while concurrently decreasing the shock-sensitivity of the metal and glass junction. The entire length of glass tubing extending outside the cabinet, connecting the reactor to the vacuum line (Fig. 5, part C), is sheathed in black opaque plastic wrap as far as its marias to protect the operator from UV light escaping via the glass. All electrical wires located inside

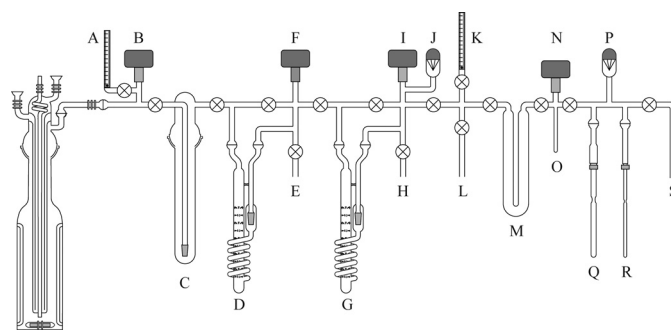


Fig. 6. DOC vacuum line. The majority of the line is manufactured from 12 mm OD standard wall Pyrex tubing, sectioned by 4 mm bore all-glass high vacuum stopcocks (QBI Corp.). Individual components are connected by spherical joints with Viton o-rings. (A) flow meter #1, (K) flow meter #2; (B), (F), (I), (N) capacitance manometers; (J), (P) thermocouple pressure gauge sensors; (C) KI solution trap; (D) modified Horibe trap #1 (dry ice/isopropanol slush bath); (G) modified Horibe trap #2 (liquid nitrogen bath); (M) U-tube trap; (O) calibrated volume with a 7 mm OD, 7 cm long cold-finger; (Q), (R) breakseal tubes for ^{14}C and ^{13}C splits, respectively, secured by internally-threaded o-ring adapters with Teflon bushings; (E), (H), (L), and (S) are conduits of a manifold (not shown for clarity) leading to the vacuum pump.

the reactor are covered with aluminum foil to retard photochemical degradation of their shielding.

The cabinet was designed to contain the water held by the reactor and recirculating chiller in the event of catastrophic failure. For protection against electrical shock, the cabinet is grounded through an all-weather, single gang outlet box installed inside the cabinet. This outlet, the magnetic spin plate that it powers, and the lower lamp terminal are elevated from the cabinet floor to prevent electrical contact with standing water. Further protection is provided by a readily accessible, clearly labeled circuit breaker located far away from the reactor for shutting down the power supply in an emergency.

Access to the interior is provided by a large, curved, hinged door with at least 2 cm of flashing around its perimeter. The flashing seals against a UV-resistant closed cell foam rubber gasket to contain light when closed securely with pawl latches. A small polycarbonate welder's lens (Sightech Lens, shade #12) on the door provides a window for safe observation of the reactor during irradiation.

DOC vacuum line—The vacuum line employed (Fig. 6) was similar to that reported by (Williams and Gordon 1970), with the following modifications. Chlorine and bromine gas produced during irradiation of seawater were removed by bubbling through a solution of 60 g potassium iodide dissolved in 150 mL of pre-irradiated Milli-Q water acidified with 1.5 mL of 85% H_3PO_4 . Water and CO_2 were condensed inside Horibe traps (Horibe et al. 1973) redesigned to fit within a standard 70 mm ID dewar flask. To compensate for their smaller volume, the surface area of the inlet stem was increased with vigreux indentations, and the traditional fritted disc was replaced with

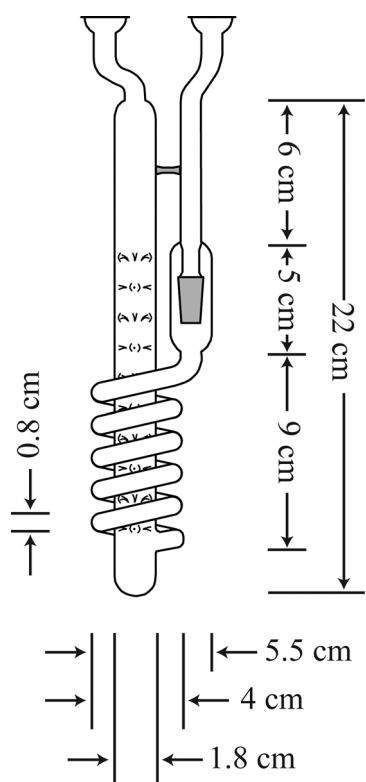


Fig. 7. Modified glass Horibe trap. Parallel 18/9 SJ sockets, allowing easy removal of the trap from the vacuum line, are splayed to accommodate the extra width of pinch clamps. The trap is mechanically strengthened by stabilizing the two stems with a solid glass strut (shown in gray).

a medium porosity fritted bubbler encased in a cylindrical bulb (Fig. 7).

The choice of deviating from previously published methods (Bauer et al. 1998a; Druffel et al. 1989; Williams and Gordon 1970) in using helium as a carrier gas is based on its extremely high vapor pressure at liquid nitrogen temperatures (-196°C) compared with those of nitrogen and oxygen (Lide 1995). This property circumvents the known hazards of condensing N_2 or O_2 in a flow-through liquid nitrogen cooled trap where pressures elevate slightly above atmospheric (Wheeler et al. 2001) while still providing an effective means of removing CO_2 from the aqueous phase. The helium stream is plumbed from each of the flow meters to a CO_2 infrared gas analyzer (IRGA; LI-COR Inc., model LI-6252) via 1/8-inch copper tubing. Since the helium gas exiting the second flow meter is CO_2 -free, the length of copper tubing downstream acts as a CO_2 -free gas ballast. The tubing, therefore, protects the line from potential back flushing of atmospheric CO_2 during analysis, minimizing the potential for contamination, and eliminating the need for an Ascarite scrubber at this location.

The line employs a rotary vane pump (Fisher Scientific Maxima C Plus) with a molecular sieve (Welch Vacuum, Cat. No. 543950) trap, that reaches an ultimate vacuum of $20\ \mu\text{mHg}$

as measured by a thermocouple pressure gauge (Televac model B2A2). DOC samples are quantified manometrically as CO_2 in a $14.84\ \text{cm}^3$ calibrated volume using an MKS Baratron capacitance manometer (model 122AA-0100AD with PDR-D-1 digital readout). This volume, $\sim 15\ \text{cm}^3$, was chosen to accommodate the performance of the gauge over the wide range of DOC concentrations found in open-ocean and coastal waters.

DOC extraction procedure—A one-gallon jug containing filtered seawater was removed from frozen storage and rapidly melted ($\sim 45\ \text{min}$) in a hot tap-water bath. Once completely liquefied, the jug was removed from the bath, wiped clean, and the seawater homogenized through 1 min of vigorous shaking. Lastly, several small aliquots of seawater, on the order of a few milliliters, were poured out to waste to ensure that the threaded spout of the jug was clean with respect to the sample's composition.

The reactor, heat exchanger, and a Pyrex-coated magnetic spinbar were rinsed with three small aliquots of sample prior to introducing $\sim 1\ \text{L}$ to the reactor body. Sample volume was quantified (see Photochemical reactor section) preceding acidification to a pH of ~ 2.5 using $\sim 1\ \text{mL}$ of 85% H_3PO_4 , delivered by a Pasteur pipette that had previously been washed with 10% HCl, and baked to 550°C . The Pyrex magnetic spinbar was added and the heat exchanger attached via a polished (no o-ring) 65/40 SJ sealed with 85% H_3PO_4 . The assembled reactor was placed on a magnetic spin plate inside the reactor cabinet, and connected to the recirculating chiller, helium supply line, and the DOC vacuum line via a Pyrex tube. Seawater was then sparged of DIC via flow meter #1 for $\sim 90\ \text{min}$ with $\sim 200\ \text{mL/min}$ of ultra high purity helium that had been scrubbed of residual CO_2 with Ascarite II (20- to 30-mesh, Acros Organics). Complete removal of DIC was monitored using an infrared CO_2 analyzer. The DOC line, with the exception of the KI trap, was pumped to ultimate vacuum during this time.

To safely vent excess pressure generated within the reactor during irradiation without compromising the analysis, a dry, low-blank compartment was created as follows. After sufficiently sparging DIC from the seawater sample, both Horibe traps were isolated from the pumps and a dry ice/isopropanol slush (hereafter referred to as "slush") was placed on Horibe trap #1 (Fig. 6). The pressure gradient between the reactor and vacuum line was then reduced by carefully diverting the helium stream from flow meter #1 to flow meter #2. To prevent an eruption of helium through the KI solution, this process involved first opening the KI trap to the Horibe traps, then slowly metering helium through the stopcock upstream from the KI trap. When the pressure inside the traps finally exceeded atmospheric pressure by at least 10 Torr, the helium was vented through flow meter #2. After confirmation from the IRGA that the helium effluent was CO_2 free, both the helium regulator and stopcock below flow meter #2 were closed, leaving the traps isolated from the atmosphere, and slightly pressurized ($\sim 770\ \text{Torr}$). Lastly, liquid nitrogen was placed on Horibe trap #2 to collect any photochemically

produced CO₂ that might escape the reactor during irradiation. Addition of this cryogen thermally compressed the helium within the Horibe traps, thus drawing helium through the KI trap from the reactor and reducing its headspace pressure prior to irradiation.

The sample was irradiated for 4 h with 8°C recirculating chiller water and continuous agitation via the Pyrex magnetic spinbar. Reaction pressure stabilized to less than atmospheric within 30 min and reached a constant temperature of approximately 74°C within 1 h of lamp ignition. Following irradiation, the stopcock between the reactor and KI trap (Fig. 6) was immediately closed to prevent the thermally contracting headspace gas from siphoning KI solution back toward the reactor. The reactor was cooled with flowing air and recirculating water for an additional 5 min prior to opening the cabinet for inspection.

The irradiated seawater was again sparged with He gas (200 mL/min, ~15 psig), flowing through a series of traps to remove impurities and collect the sample CO₂. Chlorine and bromine gas were removed from the helium stream chemically by the KI trap, while water vapor was condensed in the first Horibe trap immersed in slush (-78°C). Sample CO₂ was condensed in the second Horibe trap (cooled with liquid nitrogen, -196°C), and the stripped helium was vented from the system via flow meter #2 (Fig. 6).

After sufficient sparging (~90 min at 200 mL/min as previously determined by IRGA), the second Horibe trap was isolated and pumped to ultimate vacuum. The sample was then successively distilled from this Horibe trap to the U-tube, then to the cold-finger using liquid nitrogen and slush. Following thermal equilibration of the cold-finger with ambient air, the mass of DOC in the sample was determined manometrically as CO₂. The sample was then flame-sealed inside 9 mm OD Pyrex break-seal tubes for accelerator mass spectrometry (AMS) analysis of both Δ¹⁴C and δ¹³C. From samples containing more than 400 μgC, approximately 250 μgC was split and flame-sealed into 6 mm OD break-seal tubes for higher precision δ¹³C measurement by isotope ratio mass spectrometry (IRMS, Finnigan Delta-Plus). Following extraction, the first Horibe trap (Fig. 6, component D) was removed from the line and dried prior to analyzing subsequent samples. This prevented the line from becoming inundated with water vapor, minimizing the length of time and flame-off procedures necessary to regain ultimate vacuum.

Splits of CO₂ for Δ¹⁴C analyses were first converted to graphite targets on iron catalyst (Vogel et al. 1987) and then analyzed by the UCI Keck Carbon Cycle AMS (KCCAMS) facility's compact AMS system (NEC 0.5 MV 1.5 SDH-2 AMS). Splits containing less than 10 μgC were graphitized and analyzed at KCCAMS using slightly modified procedures for ultra-small samples detailed elsewhere (Santos et al. 2007). In all cases, radiocarbon analyses are reported as Δ¹⁴C, the per mil sample ¹⁴C/¹²C ratio relative to 95% of the activity, in 1950 AD, of National Bureau of Standards (NBS) oxalic acid 1 normal-

ized to δ¹³C = -19 per mil with respect to Pee Dee Belemnite (Stuiver and Polach 1977). Seawater Δ¹⁴C measurements were corrected for decay since the time of sampling, and normalized using ¹³C/¹²C ratios measured by the AMS during the routine ¹⁴C/¹²C analyses.

Because the DOC certified reference material was collected aboard the R/V *Weatherbird*, on which tracer studies have been performed, the potential risk of contamination precluded its use in assessing this method. Rather, standard additions were performed to determine the extent of oxidation, collection efficiency, and preservation of isotopic signature during analyses. The following isotopic standards were chosen based on their importance in radiocarbon analyses and the range of Δ¹⁴C values that they encompass: NBS oxalic acid 1 (HOx1; NIST-SRM-4990B), NBS oxalic acid 2 (HOx2; NIST-SRM-4990C), International Atomic Energy Agency (IAEA) C-6 (i.e., ANU sucrose), and IAEA C-7 (i.e., oxalic acid). Grains of these standards were massed on weighing paper with an electronic microbalance (Mettler Toledo AG204, ± 0.1 mg), directly transferred to pre-irradiated Milli-Q or seawater inside the reactor, and processed by the same general procedure above. Standard additions were also performed to determine the blank isotopic signature by mass balance because the mass of background carbon was too small for direct AMS measurement. Assuming that the CO₂ collected during any extraction was composed only of that in the sample and that of a reproducible blank, all isotope ratios were blank corrected accordingly with propagation of corresponding errors (Hayes 2002; Hwang and Druffel 2005; Pearson et al. 1998).

Assessment

General performance—The lowest backgrounds, consistently ~ 2 μg C, were obtained through re-irradiation of samples and Milli-Q water. Therefore, following the UV extraction of a sample, the reactor need only be rinsed as stated in the general procedure to prepare for irradiation of the next sample. This procedure minimizes the chemicals, energy, and time that would otherwise be expended through acid washing and baking the reactor between analyses. Furthermore, quartz glass superficially cleaned is susceptible to hazing during repeated high temperature baking. Therefore, compared with chemical washing and baking, the UV cleaning technique should also prolong the optical clarity and useful lifetime of the reactor body.

The blank of a prototype of the reactor shown in Fig. 1, employing Tygon tubing to deliver helium, was reduced from 41 to 15 μgC per liter of sample with the addition of marias (Fig. 3). Replacing Tygon with copper tubing in the current design practically eliminated leakage of CO₂ into the system, resulting in the lowest background carbon concentration for DOC measurements, ~0.2 μM. In absence of igniting the UV lamp, full analyses of pre-irradiated Milli-Q water did not produce detectable quantities of CO₂, suggesting that the majority of blank carbon was generated from oxidizable organic matter rather than the introduction of CO₂ from the UHP

Table 1. DOC system performance on standards and seawater

Analyte	n	[DOC] (μM)	$\pm 1\sigma$ (μM)	$\Delta^{14}\text{C}$	$\Delta^{14}\text{C}$	$\pm 1\sigma$ (‰)	$\delta^{13}\text{C}$	AMS- $\delta^{13}\text{C}$	$\pm 1\sigma$ (‰)
				expected*	mean		expected	mean	
NBS HO \times 1	3			33.1	31.1	1.9	-19.3	-20.4	1.5
IAEA C-7	6			-508.0	-509.0	2.6	-14.5	-13.1	2.9
Pulse 45, 20 m									
~1 L samples	3	71.8	1.5		-302.1	2.0		-23.0	1.5
0.5 L dilution	1	71.7			-303.5	1.4		-20.9	0.2
Pulse 45, 2013 m	2	39.2	0.5		-579.5	1.7		-17.5	7.5

*The expected IAEA C-7 $\Delta^{14}\text{C}$ value was calculated from the fraction modern consensus value (Le Clercq et al. 1998) as a geochemical sample without age correction (Stuiver and Polach 1977) measured in 2006.

helium or leaks into the vacuum line. The most likely carbon sources are, therefore, contributions from organic contamination present in the system prior to irradiation and that which may be introduced by UHP helium during the DIC sparge.

Standard additions (Table 1), ranging from 12 $\mu\text{g C}$ to 3.4 mg C, were recovered with an average yield of $98.2 \pm 5.4\%$ ($n = 12$, ± 1 standard deviation of the mean). The $\Delta^{14}\text{C}$ signatures of the photo-mineralized standards were highly reproducible and agreed well with consensus values. Replicate analyses of seawater demonstrate highly reproducible measurements of DOC concentration and isotope ratios in natural samples. The concentration measurements of these samples were within the range of seasonal variability previously reported for each depth layer (1 μm filter; 20-25 m, and 1500-2500 m) from Station M between July 1991 and June 1995 (Bauer et al. 1998a, 1998b). Although direct comparison is complicated by the different DOC size fractions analyzed and the additional time that has passed since the global radiocarbon spike derived from nuclear weapons testing in the 1950s and 1960s, $\Delta^{14}\text{C}$ measurements were within the range of previously reported seasonal variability ($\leq \pm 2\sigma$ of the mean historic values of each depth layer). Therefore, in addition to the accurate and precise measurements of concentrations and isotope ratios obtained for standards, reproducible and historically consistent measurements of seawater substantiate this method as a means to quantitatively extract marine non-volatile DOC with isotopic fidelity.

The range of masses analyzed in standard additions demonstrated that this system reliably extracted solutions with concentrations as low as 1 μM . These concentrations can be produced analogously by diluting 30 mL of 33 μM deep seawater into 1 liter of pre-irradiated acidified Milli-Q water, with a total DOC mass equal to six times the new background. Assuming a detection limit equal to twice the background, this method could theoretically extract 4 $\mu\text{g DOC}$, equivalent to 10 mL of deep seawater. These volumes represent a significant decrease in detection limit from the 650 mL of seawater previously required for marine DOC $\Delta^{14}\text{C}$ measurements.

Analysis of a 500-mL seawater sample diluted to 1 L with pre-irradiated acidified Milli-Q water produced concentration and $\Delta^{14}\text{C}$ values statistically indistinguishable from pure seawater

samples (Table 1). However, the analytical performance on diluted samples approaching the new detection limit is subject to the following considerations. First, the accuracy of sample volume measurements using the calibrated reactor decreases, thereby increasing the uncertainty of concentration determinations. This limitation does not affect $\Delta^{14}\text{C}$ determinations, and can be mitigated by measuring the concentration of a second aliquot with an alternative method, such as high temperature combustion (Sharp 2002). Second, although AMS analysis is now possible on samples containing as little as 2 μgC (Santos et al. 2007), the $\Delta^{14}\text{C}$ uncertainty of ultra-small samples is greater than for larger samples. Third, AMS and IRMS are destructive techniques, each requiring a minimum amount of non-reusable carbon, and the mass of carbon contained within 30 mL of seawater is insufficient for both analyses. However, at the expense of finer precision, $\delta^{13}\text{C}$ can still be quantified during routine $\Delta^{14}\text{C}$ measurements at KCCAMS and other facilities with similar AMS systems. Fourth, as the ratio of sample carbon to blank carbon approaches unity, meticulous blank corrections become vital for accurate isotopic measurements. Lastly, the time required to perform these analyses nearly doubles with the pre-irradiations required for low blanks. Despite these considerations, the dilution technique provides a means for measuring $\Delta^{14}\text{C}$ in samples that were previously impossible or overwhelmingly challenging.

Some seawater samples were resistant to graphitization, demonstrating a substantially longer time to completion than standards oxidized in Milli-Q water. Preliminary chromatographic analyses (Colman et al. 2001) of sub-sampled CO_2 revealed traces (< 100 ppb) of methyl halides. These compounds were not detected in the Ascarite scrubbed helium gas. Therefore, they are likely additional photochemical products derived partly from salts, and may have been responsible for inhibiting graphitization. Samples demonstrating this phenomenon were graphitized by initially bringing the ovens to temperature, prematurely terminating the procedure, and cooling to room temperature, followed by resuming graphitization with standard operating procedures. Analytically, these impurities do not interfere with manometric quantification since they are small molecules, stoichiometrically equivalent

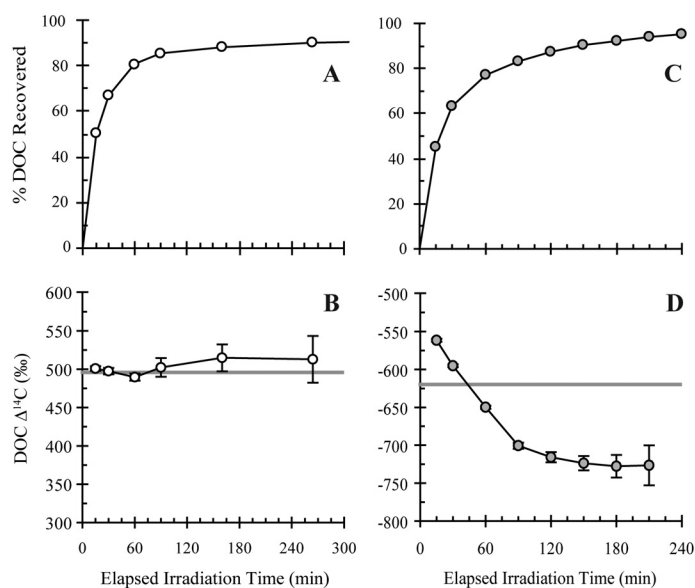


Fig. 8. Time series showing (A) the percent DOC cumulatively collected with each successive irradiation and (B) blank-corrected $\Delta^{14}\text{C}$ signatures of the individual irradiations for a $\sim 104 \mu\text{M}$ solution of IAEA C-6 (ANU sucrose) dissolved in pre-irradiated Milli-Q water; (C) the percent DOC cumulatively collected and (D) blank-corrected $\Delta^{14}\text{C}$ values of 2007 m seawater, (Station 4506, $34^\circ 55.06' \text{ N}$, $123^\circ 11.91' \text{ W}$, 27 October 2004). The gray line in (B) represents the known $\Delta^{14}\text{C}$ value of IAEA C-6, calculated from the fraction modern consensus value (Rozanski et al. [1992] as a geochemical sample without age correction (Stuiver and Polach 1977) measured in 2006. The concentration obtained ($44.2 \mu\text{M}$) from a single, continuous 4-h irradiation on a separate aliquot of the same seawater sample was used to determine the percent DOC recovered, with the corresponding $\Delta^{14}\text{C}$ value shown in (D) as the gray line. Error bars represent $\pm 1\sigma$ propagated through blank-correction. $\Delta^{14}\text{C}$ values in (B) were corrected with a mass balance determined blank $\Delta^{14}\text{C}$ value derived from a micro-addition of 0.026 mg IAEA C-6 (i.e., $\sim 13 \mu\text{gC}$) massed on a microbalance (Sartorius M2P, standard deviation = $\pm 0.001 \text{ mg}$). $\Delta^{14}\text{C}$ values in (D) were measured prior to having access to a micro-balance of sufficient resolution and were blank corrected using the average $\Delta^{14}\text{C}$ value of time points between 300 and 330 (not shown) min that yielded masses of carbon within error of the re-irradiation blank.

to CO_2 with respect to carbon, and present in trace amounts. Furthermore, $\Delta^{14}\text{C}$ measurements of HOx1 diluted into seawater were statistically indistinguishable from those aliquots diluted into Milli-Q water. Therefore, marine DOC samples exhibiting graphitization inhibition were not suspected of compromised $\Delta^{14}\text{C}$ measurements.

Time series—Time series irradiations were performed to observe the evolution of photochemically mineralized DOC and its isotopic signature during the course of a full-length irradiation. Individual samples were repeatedly subjected to brief irradiations, the products of which were collected and analyzed according to the general procedure.

Analysis of IAEA C-6 sucrose dissolved in pre-irradiated Milli-Q water ($\sim 104 \mu\text{M}$ C) was consumed approximately exponentially with a 15-min half-life (Fig. 8A). The cumulative yields for these experiments were significantly less than

100%, an artifact not observed during continuous 4 h irradiations (see above) likely attributable to a small proportion of volatile compounds (e.g., CH_2O , CO) produced by incomplete oxidation of more complex molecules/moieties during the brief irradiations. Such molecules would escape each collection during sparging if their vapor pressures were sufficiently low to condense inside the slush trap, or sufficiently high to escape the liquid nitrogen trap. Furthermore, the apparent elapsed time accumulates lamp warm-up with each successive irradiation, giving the appearance of slower kinetics than for a single 4 h irradiation. The blank corrected values indicate that little, if any, apparent $\Delta^{14}\text{C}$ fractionation of this single molecule solution occurred during the course of these experiments (Fig. 8B).

Time-series irradiations of 2007 m seawater ($44.2 \mu\text{M}$) also demonstrate approximately first order DOC remineralization with a 15-min half-life (Fig. 8C). Given the different chemical nature of these two samples, the observed rate of photochemical remineralization suggests the method is kinetically limited by reactor design and total concentration of organic matter. In contrast to the standard addition, $\Delta^{14}\text{C}$ of bulk seawater becomes significantly depleted as the reaction progresses. Analytically, the mass of carbon collected in the last 30 minute of a 4-h irradiation represents $\sim 1\%$ of the bulk DOC, implying that continuous 4-h irradiation measurements of concentration and isotope ratio are insensitive to complete oxidation, despite a large shift in $\Delta^{14}\text{C}$ values.

Feasibility—The system presented here was assembled entirely from recycled components, with the exception of the UV lamp and associated power supply. Furthermore, the reactor cabinet was constructed completely from materials available at local hardware stores for $\sim \$100$, reducing the construction cost from a machine shop estimate of $\sim \$1,000$. The hazards associated with vacuum technology required contracting a skilled glassblower to fabricate the vacuum line and glass reactor. This custom blown glassware, in addition to the lamp, power supply, pressure gauges, flow meters, recirculating chiller, and vacuum pump would be the greatest costs for manufacturing a new system, totaling less than $\$15,000$. By itself, the IRGA used in this work costs an additional $\$15,000$, but could be substituted with a less sensitive model for less than one third of that price.

Safe operation of the system described above requires basic knowledge of vacuum chemistry, UV technology, heat transfer, and respect for their limitations and associated hazards. Such information is available from health and safety offices, lamp manufacturers, textbooks, and experienced technicians.

Discussion

The greatest challenges for measuring marine DOC isotope ratios are the overwhelming proportion of salts, high blanks, and limited quantities of irreplaceable samples. These challenges have confined successful and important measurements to a limited number of laboratories, representing the bulk of

the community's oceanographic DOC $\Delta^{14}\text{C}$ knowledge for more than 30 years. While the principles of photochemical oxidation employed in our system have been previously published in textbooks and scientific papers, detailed accounts of the construction and safe operation of such systems serving this application have not. The materials and methodology herein are intended to serve the community with a reproducible base upon which successive systems can be designed and improved, enabling and encouraging more analyses.

Historically, the questions subsequently examined through this evolving methodology were posed knowing the inherent restrictions of detection limits and blanks, with the knowledge gained becoming a cornerstone of marine organic biogeochemistry. The methods and instruments described above have shown improvements in the analytical blank and precision of marine non-volatile DOC isotope ratio measurements while at the same time reducing risks to the instrument operator. Furthermore, this methodology represents an important step forward in reducing the minimum sample size required for accurately measuring marine DOC isotope ratios, enabling measurements of carbon isotope ratios that were previously overwhelmingly challenging. In general, such organic samples may be of low geochemical abundance, obtained in low yields after processing, require minimally invasive sampling to avoid methodological artifacts, or where increased sub-sampling (e.g., for additional complementary measurements or finer time-resolved analyses) is desired in systems otherwise constrained. Some possible examples include simplified porewater (Bauer et al 1995; Chasar et al 2000; Wassenaar et al 1990) analyses, observing rainwater DOC concentration and isotope ratio (Raymond 2005) evolve during a storm or brief shower, determining groundwater organic carbon fluxes and/or aquifer residence times (Burr et al. 2001), monitoring the organic content of fluids within or pumped through organisms (Yahel et al. 2003) isotopically, or sub-sampling vent waters to complement a suite of chemical analyses with $\Delta^{14}\text{C}$ and $\delta^{13}\text{C}$ measurements. Successful analyses of diluted seawater suggest that, with further testing, this reactor may also be useful in processing pure freshwater samples. However, the manometric calibrated volume should be redesigned to accommodate the anticipated range in freshwater DOC concentrations. Furthermore, time series irradiations of concentration would be required to determine an appropriate irradiation time for quantitative DOC oxidation.

Geochemically, the time series irradiations suggest that deep marine DOC is kinetically heterogeneous, and composed of molecules that span a continuum of susceptibility to photochemical remineralization. The quantities and isotopic signatures of each component cannot be extracted from the time series in Fig. 8 easily, because it represents the superposition of every component's photochemical remineralization curves. Furthermore, the radiant source used in these experiments was not a solar simulator and the information obtained cannot be directly extrapolated to photochemical remineralization in

natural waters by sunlight. However, the experiments reveal a continuum that appears to co-vary with $\Delta^{14}\text{C}$, consisting of enriched and labile components as well as depleted and recalcitrant components relative to bulk measurements. While recent evidence suggests the existence of variably aged marine DOC components (Loh et al. 2004), the photochemical labilities of these components have not been established. Further study may resolve the importance of photochemical remineralization to the observed oceanic distribution of DOC concentrations and isotope ratios.

Comments and recommendations

Incorporating baffled air intakes noticeably reduced the amount of light escaping the reactor cabinet, and is recommended for any system that employs lamps with hazardous output in need of ventilation. Keeping the basic principle of a tightly folded path, their dimensions can be easily customized to accommodate virtually any desired flow rate or trajectory through a system. Incorporating these devices into photochemical systems, in addition to using personal protective gear, will greatly reduce operator exposure to UV light.

The UV output of medium pressure mercury lamps eventually decreases with use, concomitantly degrading the reactor system's efficacy. Therefore, standard additions and blank measurements should be performed routinely, not only as a complement to seawater analyses, but also as a metric for system performance and criterion for lamp replacement. Lamp lifetime estimates range from 1000 to 2000 h when mounted in an ideal horizontal orientation, with an effective aging of approximately 1 h for each ignition in addition to the number of hours illuminated (UV Doctor, pers. comm.). The vertical orientation necessary for the reactor results in asymmetric heating of the electrodes and is expected to decrease the effective lifetime of the lamp. Although this effect has not yet been evaluated, the lamp used in this study has effectively aged 477 h without requiring adjustment to the length of each irradiation for successful sample extraction.

Disregarding breakage, the most appropriate metric for the glass reactor life expectancy is a significant decrease in system performance that requires procedural modification, reactor repair, or replacement. This reactor has not observably deviated from its initial performance after 135 uses. The practical life expectancy has not been quantified or further projected. However, it is most susceptible to degeneration from (1) developing leaks through the large spherical joint or (2) decreasing transmittance of the quartz body. The following considerations of these potential sensitivities may prolong the reactor's service. Firstly, leaks resulting from scratches on mating surfaces of the joint could be ameliorated through regrinding. The risk of developing leaks through warping the joint by overheating is practically eliminated since routine baking is no longer necessary to obtain low blanks. Secondly, decreasing transparency may result from exposing inadequately cleaned surfaces (e.g., from fingerprints) to light or heat, gradual

inorganic fouling of the quartz-water interface (Lin et al. 1999), or light-induced transmission losses known as solarization (Möncke and Ehrt 2004; Wood and Leathwood 1929). A clean external surface is easily maintained through wearing gloves, frequent inspections, and removing any grime prior to irradiation. Inorganic fouling has not yet been observed, but could potentially be removed with strong acid (e.g., HCl or aqua regia) if necessary. Solarization, however, is a chemical change within the glass matrix dependent upon the presence of non-silica constituents and radiant exposure. Such transmission losses are therefore difficult to control, but have been observed to reach a steady state in several glasses following an initial period of seasoning (Stockbarger and Johnson 1930; Wood and Leathwood 1929). The length of this period and the degree of solarization have not been quantified in this reactor.

References

- Armstrong, F. A. J., P. M. Williams, and J. D. H. Strickland. 1966. Photo-oxidation of organic matter in sea water by ultraviolet radiation, analytical and other applications. *Nature* 211:481-483.
- Bauer, J. E., E. R. M. Druffel, P. M. Williams, D. M. Wolgast, and S. Griffin. 1998a. Temporal variability in dissolved organic carbon and radiocarbon in the eastern North Pacific Ocean. *J. Geophys. Res.* 103:2867-2881.
- , ———, D. M. Wolgast, S. Griffin, and C. A. Masiello. 1998b. Distributions of dissolved organic and inorganic carbon and radiocarbon in the eastern North Pacific continental margin. *Deep-Sea Res. II* 45:689-713.
- , C. E. Reimers, E. R. M. Druffel, and P. M. Williams. 1995. Isotopic constraints on carbon exchange between deep ocean sediments and sea water. *Nature* 373:386-389.
- , P. M. Williams, and E. R. M. Druffel. 1992. Carbon-14 activity of dissolved organic carbon fractions in the north-central Pacific and Sargasso Sea. *Nature* 357:667-670.
- Burr, G. S., and others. 2001. Sample preparation of dissolved organic carbon in groundwater for AMS C-14 analysis. *Radiocarbon* 43:183-190.
- Chasar, L. S., J. P. Chanton, P. H. Glaser, D. I. Siegel, and J. S. Rivers. 2000. Radiocarbon and stable carbon isotopic evidence for transport and transformation of dissolved organic carbon, dissolved inorganic carbon, and CH₄ in a northern Minnesota peatland. *Global Biogeochem. Cycles* 14:1095-1108.
- Colman, J. J., A. L. Swanson, S. Meinardi, B. C. Sive, D. R. Blake, and F. S. Rowland. 2001. Description of the analysis of a wide range of volatile organic compounds in whole air samples collected during PEM-Tropics A and B. *Anal. Chem.* 73:3723-3732.
- Druffel, E. R. M., and others. 1989. Radiocarbon in dissolved organic and inorganic carbon from the Central North Pacific. *Radiocarbon* 31:523-532.
- Hammesfahr, J. E., and C. L. Strong. 1968. Creative glassblowing. W. H. Freeman and Company.
- Hayes, J. M. 2002. Practice and principles of isotopic measurements in organic geochemistry [lecture notes, 2nd revision, August, 2002]. <<http://www.nosams.whoi.edu/docs/IsoNotesAug02.pdf>>. Accessed March 2006.
- Hedges, J. I. 1992. Global biogeochemical cycles: progress and problems. *Mar. Chem.* 39:67-93.
- Horibe, Y., K. Shigehara, and Y. Takakuwa. 1973. Isotope separation factor of carbon dioxide-water system and isotopic composition of atmospheric oxygen. *J. Geophys. Res.* 78:2625-2629.
- Hwang, J., and E. R. M. Druffel. 2005. Blank correction for ¹⁴C measurements in organic compound classes of oceanic particulate matter. *Radiocarbon* 47:75-87.
- Le Clercq, M., J. van der Plicht, and M. Groning. 1998. New C-14 reference materials with activities of 15 and 50 pMC. *Radiocarbon* 40:295-297.
- Lide, D. R. 1995. CRC handbook of chemistry and physics, special student edition. Chemical Rubber Publishing Company.
- Lin, L.-S., C. T. Johnston, and E. R. Blatchley III. 1999. Inorganic fouling at quartz: water interfaces in ultraviolet photoreactors—I. chemical characterization. *Water Res.* 33:3321-3329.
- Loh, A. N., J. E. Bauer, and E. R. M. Druffel. 2004. Variable aging and storage of dissolved organic components in the open ocean. *Nature* 430:877-881.
- Meybeck, M. 1982. Carbon, nitrogen, and phosphorus transport by world rivers. *Am. J. Sci.* 282:401-450.
- Meyers-Schulte, K. J., and J. I. Hedges. 1986. Molecular evidence for a terrestrial component of organic-matter dissolved in ocean water. *Nature* 321:61-63.
- Möncke, D., and D. Ehrt. 2004. Irradiation induced defects in glasses resulting in the photoionization of polyvalent dopants. *Opt. Mater.* 25:425-437.
- Opsahl, S., and R. Benner. 1997. Distribution and cycling of terrigenous dissolved organic matter in the ocean. *Nature* 386:480-482.
- Pearson, A., A. P. McNichol, R. J. Schneider, K. F. Von Reden, and Y. Zheng. 1998. Microscale AMS C-14 measurement at NOSAMS. *Radiocarbon* 40:61-75.
- Raymond, P. A. 2005. The composition and transport of organic carbon in rainfall: Insights from the natural (¹³C and ¹⁴C) isotopes of carbon. *Geophys. Res. Lett.* 32:L14402 1-4.
- Rozanski, K., and others 1992. The IAEA ¹⁴C intercomparison exercise 1990. *Radiocarbon* 34:506-519.
- Santos, G. M., J. Southon, S. Griffin, S. R. Beaupré, and E. R. M. Druffel. 2006. Ultra small-mass ¹⁴C-AMS sample preparation and analysis at the KCCAMS Facility. *Nucl. Instr. Meth. Phys. Res. B.*
- Sharp, J. H. 2002. Analytical methods for total DOM pools, p. 35-58. *In* D. A. Hansell and C. A. Carlson [eds.], *Biogeochemistry of marine dissolved organic matter*. Academic Press.
- Smith, K. L., and E. R. M. Druffel. 1998. Long time-series monitoring of an abyssal site in the NE Pacific: an introduction. *Deep-Sea Res. Part II* 45:573-586.

- Stockbarger, D. C., and L. B. Johnson. 1930. Comparison between artificial and natural solarization and stabilization of special ultraviolet transmitting glasses commercially on the market. *J. Frank. Inst.* 210:455-459.
- Stuiver, M., and H. A. Polach. 1977. Discussion: Reporting of ^{14}C data. *Radiocarbon* 19:355-363.
- Vogel, J. S., D. E. Nelson, and J. R. Southon. 1987. ^{14}C background levels in an accelerator mass spectrometry system. *Radiocarbon* 29:323-333.
- Wassenaar, L. I., M. J. Hendry, R. Aravena, and P. Fritz. 1990. Organic carbon isotope geochemistry of clayey deposits and their associated porewaters, southern Alberta. *J. Hydrol.* 120:251-270.
- Wheeler, M. D., C. A. Rocger, and J. E. Kyla. 2001. Cryogenic liquids and the scientific glassblower. *Fusion J. AM. Sci. Glassblowers Soc.* 48:25-31.
- Williams, P. M. 1968. Stable carbon isotopes in the dissolved organic matter of the sea. *Nature* 219:152-153.
- and E. R. M. Druffel. 1987. Radiocarbon in dissolved organic matter in the central North Pacific Ocean. *Nature* 330:246-248.
- and L. I. Gordon. 1970. Carbon-13: carbon-12 ratios in dissolved and particulate organic matter in the sea. *Deep-Sea Res.* 17:19-27.
- H. Oeschger, and P. Kinney. 1969. Natural radiocarbon activity of dissolved organic carbon in North-East Pacific Ocean. *Nature* 224:256-258.
- Wood, A. R., and M. N. Leathwood. 1929. Glasses transparent to ultra-violet radiation. *Nature* 124:441-442.
- Yahel, G., J. H. Sharp, D. Marie, C. Häse, and A. Genin. 2003. In situ feeding and element removal in the symbiont-bearing sponge *Theonella swinhoei*. Bulk DOC is the major source for carbon. *Limnol. Oceanogr.* 48:141-149.

Submitted 21 June 2006

Revised 30 November 2006

Accepted 15 December 2006